Molecular dynamics simulations of $\langle 1\,0\,\bar{1}\,0\rangle/\psi$ tilt grain boundaries in ice

2016 Modelling Simul. Mater. Sci. Eng. 24 045015

(http://iopscience.iop.org/0965-0393/24/4/045015)

IOP Publishing Modelling and Simulation in Materials Science and Engineering

Modelling Simul. Mater. Sci. Eng. **24** (2016) 045015 (10pp) doi:10.1088/0965-0393/24/4/045015

Molecular dynamics simulations of $\langle 1\,0\,\bar{1}\,0\rangle/\psi$ tilt grain boundaries in ice

C L Di Prinzio and R G Pereyra

FAMAF (Facultad de Matemática Astronomía y Física, Universidad Nacional de Córdoba), Medina Allende y Haya de la Torre. Ciudad Universitaria (5000), CONICET (Consejo Nacional de Ciencia y Tecnología), Ciudad Universitaria, Córdoba (5000), Argentina

E-mail: carlosdiprinzio@gmail.com

Received 29 June 2015, revised 8 March 2016
Accepted for publication 4 April 2016
Published 25 April 2016

Abstract

In this paper, molecular dynamics simulations (MDS) of $\langle 1\,0\,\bar{1}\,0\rangle/\psi$ symmetric tilt ice grain boundaries are presented. The MDS were carried out using the GROMACS v4.5.5 program, and the water molecules were described using the TIP5P-Ew model. The grain boundary energies, γ_{gb}, relative to those of the surface free energies, γ_s, were obtained as a function of the misorientation angle Ψ, and compared with the γ_{gb}/γ_s values experimentally obtained. The results show a good correspondence between the experimental and simulated values. The planar density of coincidence sites at the grain boundary planes, Γ, was obtained as a function of ψ. The Γ values were compared with the simulated γ_{gb}/γ_s values and a relation between the minimum of the simulated γ_{gb}/γ_s values and the maximum of the Γ values was observed, suggesting that the CSL theory is a good starting point to detect low energy ice GBs.

Keywords: grain boundary energy, ice, GROMACS, grain boundary structure

(Some figures may appear in colour only in the online journal)

1. Introduction

Grain boundaries (GBs) determine many of the physical properties of polycrystalline materials [1]. The technological advances in both measurement devices and computer systems occurring during the last 20 years, have enormously improved our understanding of the structure and properties of most grain boundaries. Today, due to the use of new microscopes, real positions of atoms in the GBs can be revealed, and a lot of their properties can be computer-simulated [2–4].

Ice is a material that is involved in a variety of natural processes: cloud formation and transport of air pollutants [5]; glacier dynamics [6]; past climate records [7], among other processes. However, very little progress has been made in relation to the knowledge of ice GBs, especially at temperatures near the melting point. This is so because the special ice property, which currently hinders microscope ice observation at molecular level, is its high vapor pressure at temperatures higher than 200 K.

It is known that the more studied ice crystalline structure is the hexagonal structure, called Ih, since the other phases are not macroscopically present at temperatures and pressures where natural Earth processes occur [8].

To our knowledge, there are not many studies on the structure of ice GBs. Among the experimental ones, we can cite those published by Thomson *et al* [9] in which liquid GBs are observed due to the presence of high impurity concentrations; Ketcham and Hobbs [10], in which the ice GBs energies were experimentally determined; Suzuki and Kuroiwa [11], in which the energies of several GBs relative to a reference GB were determined, and our previous works [12, 13], where the grain boundary free energies relative to the surface free energies, γ_{bg}/γ_s, were determined for high purity ice and Potassium Chloride doped ice.

On the other hand, the theoretical studies we can refer to, are those showing that some GB properties, such as mobility and energy, could be explained applying the coincident site lattice (CSL) theory [14–19]. As for the simulation models of the ice structures and some of their properties, there are many molecular dynamics simulation studies [20–27], but there are none in which a GB structure is simulated. In general, most works consisted of ice-supercooled water interfaces where structural properties, and growth rates, among others properties, are studied. For example, Nada and Furukawa [20] studied interface ice growth process on basal, prismatic and $\{1\,1\,\bar{2}\,0\}$ ice planes in contact with liquid water using the six-site model. They observed that the growth velocity at the interface was larger for the $\{1\,1\,\bar{2}\,0\}$ planes than for the basal and prismatic planes, and that the reorganization of the hydrogen-bounded network occurs three-dimensionally on the prismatic and the $\{1\,1\,\bar{2}\,0\}$ planes, whereas it occurs two-dimensionally on the basal plane. This anisotropy in the growth velocity and structure was qualitatively consistent with experimental observations.

Garcia *et al* [21] presented results for the calculation of the melting temperature from the direct coexistence of the solid-liquid interface, using various water models. The authors showed, among other things, that the TIP5P-Ew model (used in this paper) provides values which most coincide with the real values, specifically, this model gives an ice simulated melting point equal to 271 ± 2 K. In 2007, Carignano [22] showed that when ice was growing from the basal plane of hexagonal ice and from the $\{1\,1\,1\}$ plane of cubic ice, a variable number of stacking faults appeared during the crystallization in agreement with most recent experimental findings.

There were also other publications where ice surfaces exposed to vacuum were studied. We can mention for example Conde *et al* [23]. These authors, using four different water models, observed the formation of a thin liquid layer at the ice surface at temperatures below the melting point, found out that the liquid layer thickness increased with temperature and observed that, for a fixed temperature, the thickness of the liquid layer decrease in the following order: the basal plane, the primary prismatic plane, and the secondary prismatic plane. These authors also observed a good reproduction of the experimental value of the liquid layer thickness near the melting point.

Other kinds of studies with ice molecular dynamic models were carried out by Pereyra and Carignano [24] and Pereyra *et al* [25]. In these two works, the authors simulated ice nanocolumns parallel to the *c* axis of hexagonal ice immersed in vacuum or in supercooled water. The water model used was the TIP5P-Ew. In vacuum case [24], it was found that the columns have

a very stable hexagonal cross-section, and the Gibbs–Thomson effect was clearly observed as the melting temperature decreases with increasing curvature. They also observed, at the interface with vapor, that the thickness of the quasi-liquid layer increases as the temperature increases. In water case [25], the authors could establish a quantitative relationship between the critical nucleus size and the temperature. This result contributed to the comprehension of homogeneous ice nucleation explaining the relative ease with which water droplets can be supercooled under controlled experiments. Li *et al* [26] studied the homogeneous ice nucleation in a wide temperature range, calculating ice nucleation rates with the same strong temperature dependence experimentally observed. To end this brief overview, we can mention a work recently published by Choi *et al* [27]. Using the TIP5P-Ew water model, they made simulations similar to [24], and found anisotropy in ice growth on basal as well as on prismatic faces.

In this small but representative list of publications from 2005 to the present, we can see that all ice studies are based on binary systems of water and ice or ice alone, and that there are no simulating works where two pieces of ice with different orientation are put together in order to simulate a GB structure.

In this paper, we present molecular dynamics simulations (MDS) of $\langle 1\,0\,\bar{1}\,0\rangle/\psi$ symmetric tilt ice GBs. The GB energies relative to those of the surface free are obtained as a function of the orientation of the adjacent crystals and then compared with the values experimentally obtained [12, 13].

To make this work clearer, we first explain, in section 2, how the initial samples used in the grain boundaries simulations were constructed; then, in section 3, the method used in the simulations is described. In section 4, the obtained simulation results are presented and discussed in comparison with the experimental ones.

2. Bicrystal construction

An example of an initial sample, $\psi/\langle 1\,0\,\bar{1}\,0\rangle$ GB with $\psi = 60°$ is shown in figure 1(a). It consists of two slabs of I_h lattice in contact, forming a symmetrical GB. As it is schematically represented in figure 1(b), each crystal slab has its crystallographic b-axes $\langle 1\,0\,\bar{1}\,0\rangle$ parallel to the GB and its c-axes $\langle 0\,0\,0\,1\rangle$, forming a $\theta = 30°$ angle with the GB plane. Crystal 1 is the reflection with respect to the GB of Crystal 2, and they form a parallelepiped box. In this way, the c-axes of the crystals form a $\psi = 2\theta = 60°$ angle.

To prepare ice systems like the one shown in figure 1 with periodic boundary conditions in all their sides, as it is needed to carry out the computer simulations, the following steps were taken:

First, an ice crystal was constructed with an oxygen atom in the coordinate origin and the $\vec{a}$, $\vec{b}$ and $\vec{c}$ axes normal to the xy, xz and yz planes respectively. The molecules were arranged in ice conformation using the Buch algorithm [28], so that all hydrogen bonds satisfied the Bernal-Fowler rules. The dimensions of the box were 6 atomic planes in the $\vec{b}$ direction and approximately 200 in the other directions.

Second, the crystal was rotated a θ angle around the $\vec{b}$ axis, and a parallelepiped crystal with faces parallel to the **xy** and **yz** planes was constructed, so that the two faces parallel to the **xy** and **yz** planes had the same crystallographic planes. The total number of molecules, N, of one crystal could vary between 720 and 2184 depending on the system size needed to fulfill the boundary periodic conditions, as well as the Bernal–Fowler rules.

Third, in order to achieve a good thermalization of the ice crystal, 1 ns molecular dynamics simulations were performed at a temperature $T = 255\,\mathrm{K}$, a pressure $P = 1$ bar, and maintaining the number of molecules constant. Once we had the thermalized crystal, we replicated

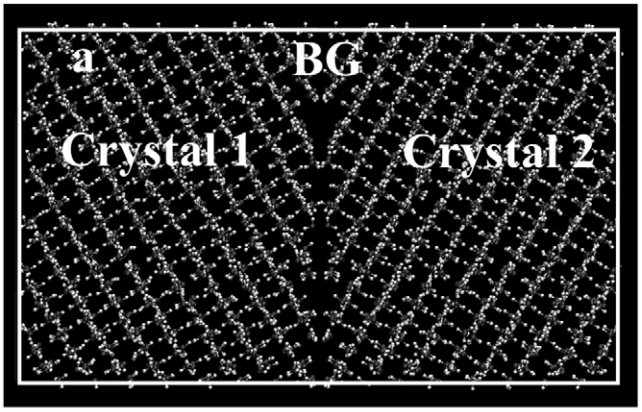

Figure 1a

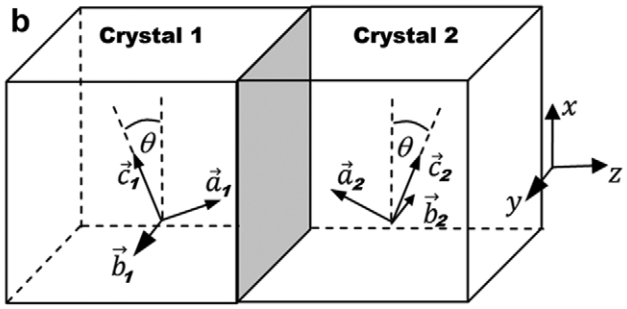

Figure 1. (a) Snapshots of an initial simulation system, corresponding to a GB misorientation $\langle 1\,0\,\bar{1}\,0\rangle/\psi$ with $\psi = 60°$ viewed from the secondary prismatic face. The grey and white spheres represent the Oxygen and Hydrogen atoms respectively. The lines indicate the limits of the parallelepiped box. (b) Scheme of the used system. $\vec{a}$, $\vec{b}$ and $\vec{c}$ are the ice crystal axes and $x.y.z$ the Cartesian axes.

the crystal making a reflection in the **xy** plane. Then, we put each crystal with their **xy** planes facing each other and separated by a water molecule diameter.

3. Computational details

The molecular dynamics simulations were carried out using the GROMACS v4.5.5 program [29]. Water molecules were described using the TIP5P-Ew model [30, 31]. This water model very well works in ice simulations, mainly because its architecture presents two sites representing the water molecule lone pairs, which contribute to form the hydrogen bonds more effectively. It also represents the liquid water surface energy very well. In fact, this program was used to calculate the surface energy of the liquid water at 300 K. Following Chen and Smith [32], the diagonal elements of the pressure tensor were used and a value of 53 mJ m^{-2} was found, which is in agreement with the values reported by these authors and with the experimental values.

The leapfrog algorithm was used for the integration of the dynamics equations, with a time-step of 0.001 ps. A spherical cut-off at 0.9 nm was imposed for the Lennard-Jones and short-range electrostatic interactions. For long-range electrostatic interactions we included corrections using the PME approach. The temperature and pressure of the system were

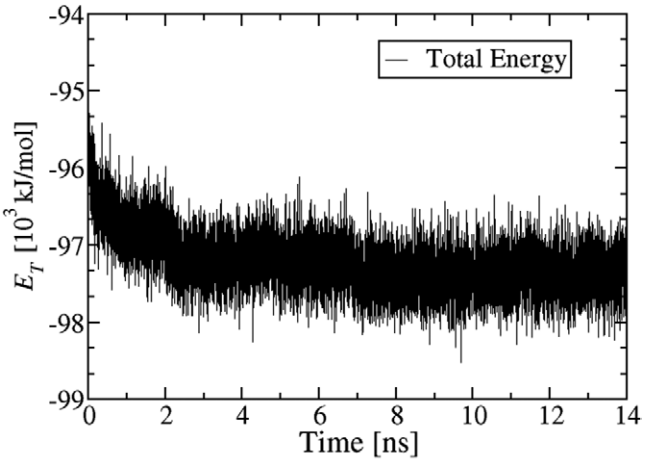

Figure 2. Time evolution of the simulated total energy corresponding to case $\psi = 2\theta = 60°$

controlled using a Nosé–Hoover thermostat and a Parrinello–Rahman barostat, respectively. Thermostat and barostat time constants were 0.5 ps approximately, and the compressibility was uniform and equal to 4.51 bar^{-1}.

The simulation times were long enough to reach a steady state. They depended on the system size and they vary between 5 and 10 ns. The time evolution of the simulated total energy (kinetics plus potential energies), corresponding to the $\psi = 60°$ case, is shown in figure 2. In this figure, it is observed that this energy starts with high values and goes to lower values until it reaches a steady state. When the system reaches this state, the total energy E_T assigned to each sample is calculated as the average of the last 1 ns values.

In order to calculate the GB energy, E_{gb}, according to [33–39], we used the following equation:

$$E_{gb} = \frac{E_T - e_{ice}n}{2d_x d_y} \tag{1}$$

Where n is the total number of water molecules, e_{ice} is the energy per molecule in the ice bulk ($e_{ice} = -45.42$ kJ mol^{-1} at $T = 255$ K and $P = 1$ bar) and $d_x d_y$ is the xy GB area. Factor 2 appears in this equation because the studied systems present two GB surfaces.

On the other hand, to obtain the surface free energy values necessary to compare our results with the experimental ones [12, 13], we performed the MDS of each of the constructed crystals in contact with vapor. We put the ice crystal in the center of a box with z-dimensions larger than those of the ice crystal, so the crystal–vapor free surfaces and the c axis formed θ angles between 0° and 90°. The z-dimension box was maintained fixed along the complete simulation time. For each studied crystal, the superficial energy E_s was calculated using the following equation:

$$E_s = \frac{E_T - e_{ice}n}{2d_x d_y} \tag{2}$$

Where $d_x d_y$ is the xy surface area. Factor 2 appears in this equation because the studied systems present two surfaces in contact with vapor.

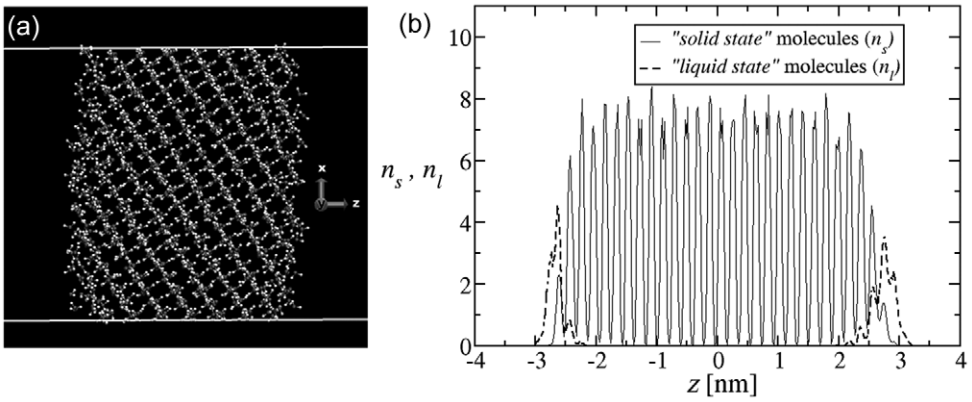

Figure 3. (a) Snapshots of a representative simulation system, corresponding to an ice slab with a free surface forming a 30° angle with the crystallographic *c*-axes, viewed from the secondary prismatic face. (b) Number of molecules in solid state liquid (black line) and in the liquid state (dashed line) as a function of z.

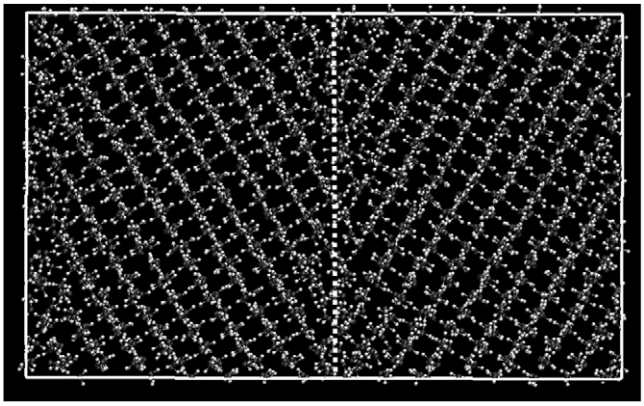

Figure 4. Final Snapshot of 60° system, corresponding to the initial GB (dash line) configuration showed in figure 1.

In figure 3(a), we present a snapshot of an ice crystal thermalized at 255 K with the same ice–vapor interface that will have an ice sample like the one shown in figure 1(a), if the surface parallel to the GB were in contact with vapor. In figure 4, it is possible to observe, at $z = \pm 3$ nm, two disordered *xy* surfaces revealing the existence of two quasi-liquid layers. This behavior is most clearly evidenced in figure 3(b), where we present the numbers of molecules in the 'solid state' (n_s) and in the 'liquid state' (n_l), calculated following the Carignano *et al* [40] method. In this method, hydrogen bonds are defined by two conditions. First, the oxygen–oxygen distance is within a 0.35 nm distance cutoff. Second, the angle formed by the hydrogen, the donor oxygen and the acceptor oxygen, is smaller than a 30° angular cutoff. Then, for each individual molecule the number of hydrogen bonds averaged during 20 ps is calculated. The molecules are considered to be in the liquid state if this number is lower than 3.3, and in the ice lattice state if it is higher. Figure 3(b) shows, in black line, the averaged in the last 1000 ps simulation time of the solid state molecular numbers present in each z-axis interval of 0.05 nm, and, in dashed line, those corresponding to the liquid state.

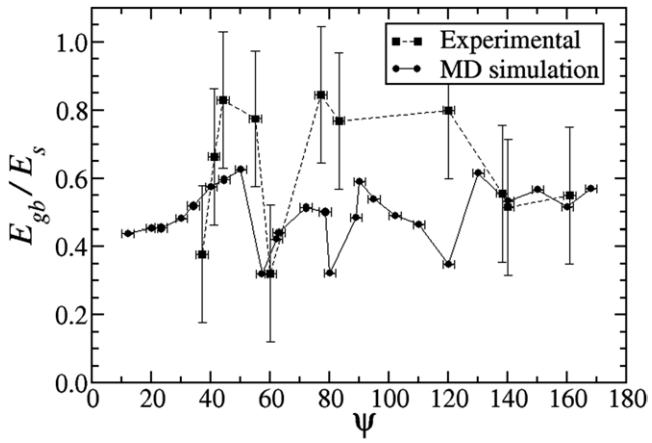

Figure 5. Values of the ratio between the energies of grain boundary (E_{gb}) and surface (E_s) calculated with MDS at 255 K and experimental values obtained by Di Prinzio *et al* [13] corresponding to $\langle 1\,0\,\bar{1}\,0\rangle/\psi$ tilt GBs.

4. Results and discussion

Figure 4 presents a snapshot of the initial configuration shown in figure 1, after a 2 ns DMS time. In this figure it is observed that, the initial GB areas free of water molecules, after a simulation time of 2 ns, are covered in general by molecules disordered with respect to the adjacent lattices.

In figure 5, the E_{gb}/E_s simulated values obtained for all the studied samples, are presented. Besides, the γ_{bg}/γ_s experimental values, obtained by Druetta *et al* [12] for symmetrical $\langle 1\,0\,\bar{1}\,0\rangle/\psi$ tilt boundaries thermalized at -18 °C, are shown. The error bars were included for computer and experimental data. The uncertainty for E_{gb}/E_s were obtained using the E_{gb} and E_s fluctuations shown in figure 3. The errors of the ψ angles used in the computer simulations were determined measuring the bicrystal misorientations after and before the simulations. The uncertainty for the γ_{bg}/γ_s and ψ experimental values were obtained from [12].

While comparing experimental and simulated values corresponding to misorientations between 30° and 90°, and between 140° and 170°, a good correspondence is noted. The agreement is not only qualitative but also quantitative; the experimental minimum at ~60° is very well reproduced by the simulation values. Note that the simulation and experimental values are almost similar, even though they may sometimes differ by a factor 2, which is of the same order of magnitude as those observed when DMS values are compared with the experimental ones.

In this figure it is also noted that, at misorientations between 90° and 140°, simulation values present minimums that are not present in the experimental values. This might not be relevant, not only because, in this range of Ψ, there are few experimental data, but also because the exact angles, at which the minimum occurs, may not have been experimentally analyzed. However, more experimental studies need to be performed in order to check this behavior more carefully.

Drueta *et al* [12] observed that the misorientations where the experimentally obtained γ_{gb}/γ_s minima occur coincide with the misorientations where the planar density of coincidence sites, Γ, are high. In order to check if all the values obtained with the DMS match this criterion, a program was conducted in order to calculate the variation of Γ as a function of ψ. In figure 6,

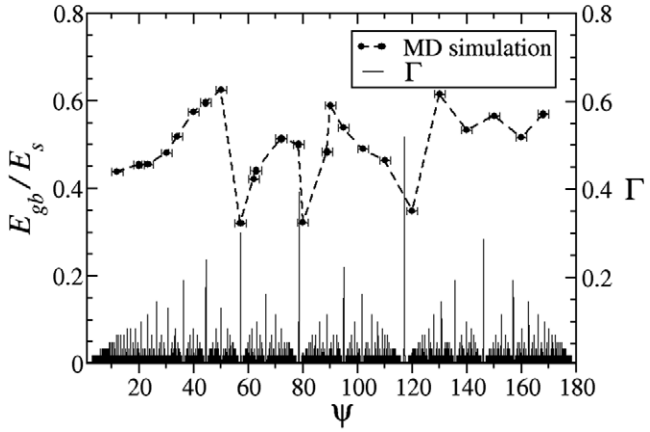

Figure 6. Values of E_{gb}/E_s calculated with MDS and of the planar density of coincidence sites at the grain boundary planes (Γ) as a function of the misorientation of the adjacent crystals, ψ.

the Γ obtained values are plotted together with the E_{gb}/E_s simulated values. This figure shows that the minima in the simulated values correspond only to Γ maxima greater than 0.3. To analyze this phenomenon the coincident sites at the GBs were studied for 23°, 34°, 44°, 57°, 63°, 78° and 88° tilt GBs which, according to González Kriegel *et al* [41], have a high density of coincidence sites. The relationship between the periodicity of simulated boundaries and the periodicity of the coincidence site array being simulated was analyzed. In all cases, except for 23° and 88° GBs, it was found that these two periodicities had an integer ratio. We should note that only the oxygen CSLs were analyzed, so the possible existence of Bjerrum defects and ionic defects could not be excluded. Finally, it should be noted that, in general, periodic structures at the GBs were not distinguished all along DMS studied time. So, we see that in ice, high Γ values are a necessary but not a sufficient condition to have low energy GBs. In the present case, only GBs with $\Gamma > 0.3$ were found to be low energy GBs, but it was not found out which special GB property causes a minimum in the GB energy. This is an issue that needs to be studied more carefully.

5. Conclusions

In this paper, $\langle 1\,0\,\bar{1}\,0\rangle/\psi$ symmetric tilt ice grain boundaries (GBs) were studied performing molecular dynamics simulations (MDS) with the GROMACS v4.5.5 program, and representing the water molecules by the TIP5P-Ew model. This investigation reveals the following:

1. The used MDS program reproduces the liquid water surface energy very well. The surface energy of the liquid water was calculated using the diagonal elements of the pressure tensor. The values found are in agreement with previously reported values.
2. The ice-vapor interfaces, simulated to obtain the surface ice energies, are molecularly disordered revealing the existence of quasi-liquid layers.
3. The E_{gb}/E_s calculated relative energies for the $\langle 1\,0\,\bar{1}\,0\rangle/\psi$ GBs with Ψ angles between 0° and 180° are in agreement with the γ_{bg}/γ_s experimental values obtained by Drueta *et al* [12]. For misorientation values between 30° and 90°, and between 140° and 170°, a very good quantitative agreement is noted, the experimental minimum at ~60° is very

well reproduced and the simulation and experimental values at most differ by a factor 2. It was also noted that, at Ψ values between 90° and 140°, E_{gb}/E_s simulation values present minimums that are not present in the experimental values and, in consequence, more experimental studies need to be performed in order to check this behavior more carefully.

4 The planar density of coincidence sites at the grain boundary planes, Γ, were computed. A relation between Γ and the simulated GB energy values was found. It was observed that the minima of the simulated values approximately coincide with the maxima of the Γ greater than 0.3. This result indicates that to find GBs with high Γ values, is a very good tool to detect low energy GBs, but it is not sufficient. Thus, the question remains: why do only GBs with Γ greater that a particular value make a low energy GBs?

Acknowledgments

This work was supported by UNC SeCyT and CONICET funds. We appreciate the technical collaboration of José Barcelona and LAMARX laboratory.

References

[1] Sutton A P and Balluffi R W 1995 *Interfaces in Crystalline Materials* (Oxford: Clarendon)
[2] Brandon D 2010 *Mater. Sci. Technol.* **26** 762–73
[3] Harmer M P 2010 *J. Am. Ceram. Soc.* **93** 301–17
[4] Mishin Y, Asta M and Li J 2010 *Acta Mater.* **58** 1117–51
[5] Pruppacher H R and Klett J D 1998 *Microphysics of Clouds and Precipitation* (Dordrecht: Kluwer)
[6] Dash J G, Rempel A W and Wettlaufer J S 2006 *Rev. Mod. Phys.* **78** 695–741
[7] Rempel A W and Wettlaufer J S 2003 *Can. J. Phys.* **81** 89–97
[8] Hobbs P 1974 *Ice Physics* (Oxford: Oxford University Press)
[9] Thomson E S, Hendrik H, Wilen L A and Wettlaufer J S 2013 *J. Chem. Phys.* **138** 124707–11
[10] Ketcham W M and Hobbs P V 1969 *Phil. Mag.* **19** 1161–73
[11] Suzuki S Y and Kuroiwa D 1972 *J. Glaciol.* **11** 265–77
[12] Druetta E, Nasello O B and Di Prinzio C L 2014 *J. Mater. Sci. Res.* **3** 69–76
[13] Di Prinzio C L, Druetta E and Nasello O B 2014 *J. Phys. Chem.* B **118** 13365–70
[14] Higashi A 1988 *Lattice Defects in Ice Crystals* (Sapporo: Hokkaido University Press) pp 129–46
[15] Di Prinzio C L and Nasello O B 1997 *J. Phys. Chem.* B **101** 7687–90
[16] Hondoh T and Higashi A 1979 *Phil. Mag.* A **31** 137–49
[17] Kobayashi T and Furukawa Y 1975 *J. Cryst. Growth* **28** 21–8
[18] Kobayashi T, Furukawa Y, Takahashi T and Uyeda H 1976 *J. Cryst. Growth* **32** 233–49
[19] Kobayashi T, Furukawa Y, Kikuchi K and Uyeda H 1976 *J. Cryst. Growth* **35** 262–8
[20] Nada H and Furukawa Y 2005 *J. Cryst. Growth* **283** 242–56
[21] García R, Fernández R G, Abascal J L and Vega C 2006 *J. Chem. Phys.* **124** 144506–11
[22] Carignano M A 2007 *J. Phys. Chem.* C **111** 501–4
[23] Conde M, Vega C and Patrykiejew A 2008 *J. Chem. Phys.* **129** 014702–11
[24] Pereyra R G and Carignano M A 2009 *J. Phys. Chem.* C **113** 12699–705
[25] Pereyra R G, Szleifer I and Carignano M A 2011 *J. Chem. Phys.* **135** 034508
[26] Li T, Donadio D, Russo G and Gali G 2011 *Phys. Chem. Phys.* **13** 19807–13
[27] Choi S, Jang R and Kim J S 2014 *J. Chem. Phys.* **140** 014701
[28] Buch V, Sandler P and Sadlej J 1998 *J. Phys. Chem.* B **102** 8641–53
[29] www.gromacs.org/
[30] Spoel D V D, Lindahl E, Hess B, Groenhof G, Mark A E and Berendsen H J C 2005 *J. Comput. Chem.* **26** 1701–18
[31] Rick S W 2003 *J. Chem. Phys.* **107** 9853–7
[32] Chen F and Smith P E 2007 *J. Chem. Phys.* **126** 221101
[33] Ikeda K, Yamada K, Takata N, Yoshida N, Nakashima H and Tsuji N 2008 *Mater. Trans.* **l49** 24–30
[34] González-Romero R L, Meléndez J J, Gómez-García D, Cumbrera F L and Domínguez-Rodríguez A 2012 *Solid State Ion.* **219** 1–10

[35] Zhang J, Zhao J and Lu J 2012 *ACS Nano* **6** 2704–11
[36] Uesugi T and Higashi K 2013 *Mater. Trans.* **54** 1597–604
[37] Movahedi-Rad A and Alizadeh R 2014 *J. Mod. Phys.* **5** 627–32
[38] Balamane H, Halicioglu R and Tiller W A 2012 *Phys. Rev.* B **46** 2250–79
[39] Somasi S and Khomami B 2004 *J. Phys. Chem.* B **108** 19721–28
[40] Carignano M A, Shepson P B and Szleifer I 2005 *Mol. Phys.* **103** 2957–67
[41] González Kriegel B J, Di Prinzio C L and Nasello O B 1997 *J. Phys. Chem.* B **101** 6243–6